# Numerical Simulation of Transient Flow of Two Immiscible Liquids in Pipeline

**Yuri V. Fairuzov**
Institute of Engineering, P.O. Box 70-472, National Autonomous University of Mexico, Mexico City 04510, Mexico

*A two-fluid model for transient flow of two immiscible liquids in a pipeline was formulated based on two transient continuity equations and a combined momentum equation in a quasi-steady form. It can be used for simulating both stratified and dispersed flow. Numerical simulations were performed to investigate the behavior of oil–water flow during transients caused by an increase or decrease in the water volume fraction at the entrance to the pipeline. An increase in the water flow rate within the stratified flow regime may result in the formation of a shock (an abrupt change in the water holdup). In transients produced by a decrease in the input water volume fraction, the smoothening of the water holdup wavefront occurs. This behavior is explained by a strong dependence of the speed of the holdup wave propagation in stratified flow on the water holdup. The results obtained for inclined pipelines show that the slope of the pipe affects the flow behavior significantly. The liquid–liquid flow model was used to simulate the transport of corrosion inhibitor in a pipeline conveying an oil–water mixture.*

## Introduction

The simulation of transient flow of two immiscible liquids in pipelines is of interest in many engineering applications. Liquid hydrocarbons transported in pipelines over long distances (for example, crude oil, gasoline, diesel) often contain free water. The presence of water in the pipeline may cause severe corrosion of the pipe walls. The internal corrosion rate depends strongly on the flow configuration of the liquid–liquid mixture (flow pattern). The most severe internal corrosion has been found to occur in pipelines in which the flow velocity is low and the phases are segregated (Ricca, 1991). Operating conditions of pipelines may vary in the time, for example, due to changes in the total flow rate or the water volume fraction (the water holdup) at the pipeline inlet. Therefore, the understanding of transient liquid–liquid two-phase flow behavior is crucial in determining the contact area of free water with the pipe walls and the time period over which this contact occurs. The water accumulation in the lower portions of pipelines, after performing ''pigging'' or ''sphering'' of the lines is another example of a transient process that should be taken into consideration in the design of oil transportation systems and their maintenance.

Continuous injection of corrosion inhibitors into pipelines is often the most economical and effective method of corrosion control (Ricca, 1991; Erickson et al., 1993). The transport and distribution of the inhibitor along the pipeline under varying operating conditions are governed by the dynamics of transient liquid–liquid flow. In order to provide the required concentration of the inhibitor at the critical locations in the line for the proper period of time, one needs to predict correctly the flow pattern and transient distributions of basic flow parameters (velocities of phases, volume fractions of phases, inhibitor concentration). The transport of corrosion inhibitor in a wet-gas pipeline has been modeled by Erickson et al. (1993). However, they do not show what governing equations have been used in their study. The inhibitor transport in unsteady liquid–liquid flow has not been investigated in the literature.

Transient gas–liquid two-phase flow has been extensively studied in the past. Comprehensive overviews of the literature in this area can be found in the works presented by Riebold et al. (1981), Wallis (1982), and Masella et al. (1998). Several computer codes, such as TRAC (Jackson, 1981), PLAC (Black et al., 1990), OLGA (Bendiksen et al., 1991), have been developed for simulating gas–liquid flows in pipelines. However, in many cases the models and methods for gas–liquid flow cannot readily be extended to liquid–liquid flow. The flow of two immiscible liquids has received little attention in the literature despite the significance of this problem. Most of the works in this area have concentrated on the analysis of the holdup, pressure drop in oil–water mixtures (Angeli and Hewitt, 1998; Trallero et al., 1995; Flores et al., 1998), and on the development of models for predicting flow regime transitions (Brauner and Maron, 1992a, b, c; Trallero, 1995).

Recently, Asheim and Grodal (1998) investigated the holdup wave propagation in vertical oil–water flow. They formulated a drift-flux model that is based on two continuity equations. The slip between phases in their mathematical formulation is predicted by a modified model of Zuber and Findlay (1965). Asheim and Grodal (1998) considered only one flow pattern, namely, the dispersion of oil in water. However, in a recently published article, Flores et al. (1998) identified six flow patterns in vertical flow. They found that the water holdup is strongly affected by the flow pattern. Transient flow of two immiscible liquids in horizontal or slightly inclined pipelines, in which the phase segregation can occur, has not been studied.

In this article, a two-fluid model for transient liquid–liquid flow in a pipeline is formulated. The model consists of two transient continuity equations and a combined momentum equation in a quasi-steady form. Wall and interfacial shear stresses are incorporated into the model in an explicit form. The model is capable of predicting the transition from segregated flow to dispersed flow. A study of transient liquid–liquid flow in a horizontal pipe is carried out. In particular, transients caused by an increase or decrease in the input volume fraction of one of the phases are analyzed. A numerical simulation of the transport of corrosion inhibitor injected into a pipeline conveying an oil–water mixture is performed.

## Model Formulation

The governing equations for transient isothermal flow of two immiscible liquids in a pipe are formulated employing the two-fluid modeling approach. The two-fluid model for isothermal liquid–liquid two-phase flow incorporates two mass conservation equations and two momentum equations. The governing equations for stratified and dispersed flow are given below.

### *Stratified flow*

For stratified flow (Figure 1), the governing equations can be written in the following form (Brauner and Maron, 1992a): Mass conservation equation for phase a

$$\frac{\partial}{\partial t}(\rho_a \alpha_a) + \frac{\partial}{\partial x}(\rho_a \alpha_a U_a) = 0. \tag{1}$$

Mass conservation equation for phase b

$$\frac{\partial}{\partial t}(\rho_b \alpha_b) + \frac{\partial}{\partial x}(\rho_b \alpha_b U_b) = 0, \tag{2}$$

where

$$\alpha_a + \alpha_b = 1. \tag{3}$$

Momentum equation for phase a

$$\frac{\partial}{\partial t}(\rho_a \alpha_a U_a) + \frac{\partial}{\partial x}(\rho_a \alpha_a U_a^2) = -\frac{\tau_a S_a}{A} - \frac{\tau_i S_i}{A} + \rho_a \alpha_a g \sin\beta - \frac{\partial}{\partial x}(\alpha_a P_a) + P_{ia}\frac{\partial \alpha_a}{\partial x}, \tag{4}$$

and for phase b

$$\frac{\partial}{\partial t}(\rho_b \alpha_b U_b) + \frac{\partial}{\partial x}(\rho_b \alpha_b U_b^2) = -\frac{\tau_b S_b}{A} + \frac{\tau_i S_i}{A} + \rho_b \alpha_b g \sin\beta - \frac{\partial}{\partial x}(\alpha_b P_b) + P_{ib}\frac{\partial \alpha_b}{\partial x}. \tag{5}$$

Assuming incompressible liquids, the continuity equations, Eqs. 1 and 2, can be rewritten as follows

$$\frac{\partial \alpha_a}{\partial t} + \frac{\partial}{\partial x}(\alpha_a U_a) = 0 \tag{6}$$

$$\frac{\partial \alpha_b}{\partial t} + \frac{\partial}{\partial x}(\alpha_b U_b) = 0. \tag{7}$$

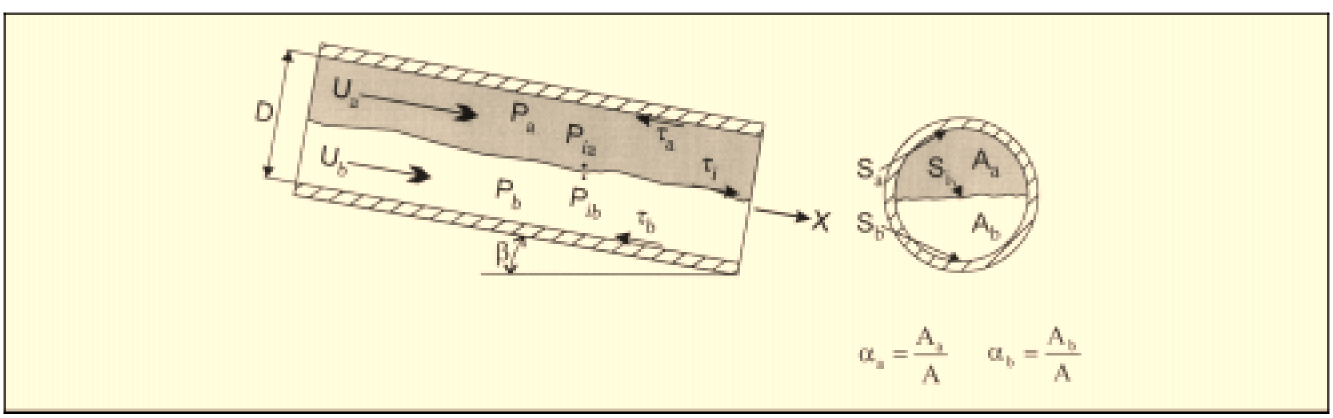


**Figure 1. Flow of two immiscible liquids in pipeline.**

Adding Eq. 6 with Eq. 7 results in

$$\frac{\partial}{\partial x}(\alpha_a U_a) + \frac{\partial}{\partial x}(\alpha_b U_b) = 0. \tag{8}$$

Examination of Eq. 8 reveals that in the flow of two incompressible immiscible liquids the sum of superficial velocities is constant along the pipeline. It is more convenient to have Eq. 8 in an integral form

$$U_a \alpha_a + U_b \alpha_b = U_m, \tag{9}$$

where $U_m$ is the mixture velocity (the total flow rate divided by the cross-section area).

The momentum equations, Eqs. 4 and 5, can be combined into a single equation as follows (Trallero, 1995):

$$\rho_b \frac{\partial U_b}{\partial t} - \rho_a \frac{\partial U_a}{\partial t} + \rho_b U_b \frac{\partial U_b}{\partial x} - \rho_a U_a \frac{\partial U_a}{\partial x} + (\rho_b - \rho_a) g \cos\beta \frac{\partial h_b}{\partial x} + \frac{\partial (P_{ib} - P_{ia})}{\partial x} = F, \tag{10}$$

where

$$F = -\tau_b \frac{S_b}{\alpha_b A} \pm \tau_i S_i \left( \frac{1}{\alpha_a A} + \frac{1}{\alpha_b A} \right) + \tau_a \frac{S_a}{\alpha_a A} + (\rho_b - \rho_a) g \sin\beta. \tag{11}$$

In slow transients, the prevailing terms in Eq. 10 are the source terms. Neglecting all remaining terms, the combined momentum equation, Eq. 10, takes the following form:

$$-\tau_b \frac{S_b}{\alpha_b} \pm \tau_i S_i \left( \frac{1}{\alpha_a} + \frac{1}{\alpha_b} \right) + \tau_a \frac{S_a}{\alpha_a} + (\rho_b - \rho_a) A g \sin\beta = 0. \tag{12}$$

Equation 12 represents a quasi-steady formulation of the combined momentum equation. Quasi-equilibrium momentum balances for both phases have been successfully used in modeling of slow transients in gas–liquid flows (Taitel and Barnea, 1997).

The model requires closure relationships for shear stresses. The wall shear stress acting on each phase is expressed in terms of the local velocity of the phase and corresponding friction factor:

$$\tau_a = f_a \frac{\rho_a U_a |U_a|}{2}, \qquad \tau_b = f_b \frac{\rho_b U_b |U_b|}{2}. \tag{13}$$

The friction factors $f_a$ and $f_b$ in Eq. 13 are evaluated using the adjustable definitions of the equivalent hydraulic diameters (Brauner and Maron, 1992a).

The interfacial stress is expressed as

$$\tau_i = f_i \frac{\rho (U_a - U_b) |U_a - U_b|}{2}, \tag{14}$$

where the interfacial friction factor is calculated using the correlation of Brauner and Maron (1992a).

### *Dispersed flow*

The liquid–liquid two-phase flow is characterized by a large momentum transfer rate. Trallero (1995) studied experimentally oil–water flow patterns in horizontal pipes. He found that the slip between phases is important only in stratified flow. In the region of dispersed flow pattern, the slip effect is negligible. Thus, in this study the dispersed liquid–liquid flow is assumed to be homogeneous

$$U_a = U_b = U_m. \tag{15}$$

In highly inclined or vertical pipes, the slip can be accounted for using a drift-flux model, such as the one proposed by Flores et al. (1998).

Thus, dispersed flow is described by the continuity equation for phase b, Eq. 7, in which the velocity of phase b is determined using Eq. 15.

Equations 7, 9, 12, or 15 form a system of equations that describe the transient flow of two immiscible liquids in a pipeline.

### *Initial and boundary conditions*

In order to complete the model formulation, one must specify initial and boundary conditions. The initial distribution of the volume fraction of phase b is assumed to be known (for example, from a steady-state model)

$$\alpha_b = \alpha_{bo}(x). \tag{16}$$

The mathematical formulation developed in this article requires specifying only one boundary condition at the entrance to the pipeline. The superficial velocities of phase b and the mixture velocity at the entrance are assumed to be known:

$$U_m = (t); \qquad U_{bs} = U_{bs,e}(t) \tag{17}$$

## Determination of Flow Pattern

A central problem in the analysis of two-phase flow is the determination of the flow pattern. Much of the past work has concentrated on the analysis of flow-regime transitions in gas–liquid two-phase flow. However, the flow-pattern prediction methods developed for gas–liquid flow cannot be readily extended to liquid–liquid systems. Some flow configurations of liquid–liquid two-phase mixtures in pipes are different from those of gas–liquid mixtures. Moreover, there is no agreement in the published literature on the classification of flow patterns in liquid–liquid flow. Trallero (1995) gives a comprehensive overview of the work done in this area.

Based on published data and his own experiments with oil–water mixtures, Trallero (1995) proposed six flow patterns (Figure 2) and classified them into two major categories:

1. Segregated flow
   - Stratified flow
   - Stratified flow with mixing at the interface
2. Dispersed flow
   - Water dominated: dispersion of oil in water and water; oil in water emulsion.
   - Oil dominated: dispersion of water in oil and oil in water; water in oil emulsion.

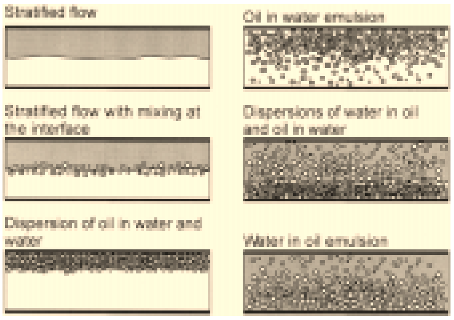


**Figure 2. Oil–water flow patterns in horizontal pipes (Trallero, 1995).**

This flow-regime classification was adopted in the present study. Here, oil is the lighter fluid.

The range of stable stratified flow is determined based on an analysis of the condition for real characteristics (well-posedness) of the (hyperbolic) governing equations, Eqs. 1–4. Relying on the well-posedness analysis carried out by Brauner and Maron (1992a), the transition from the segregated flow to dispersed flow is assumed to occur when

$$(U_b - U_a)^2 > \frac{D}{\rho_{ab}} [ (\rho_b - \rho_a) g \cos\beta + \sigma k_{rc}^2, \qquad (18)$$

where

$$\rho_{ab} = \frac{\rho_a \tilde{A}'_b}{\tilde{\rho}_a \tilde{A}_a}; \quad \tilde{\rho}_a = 1 + \frac{\rho_a \tilde{A}_b}{\rho_b \tilde{A}_a};$$

$$\tilde{A}_a = \frac{\alpha_a A}{D^2}; \quad \tilde{A}_b = \frac{\alpha_b A}{D^2}; \quad \text{and} \quad \tilde{A}'_b = \frac{S_i}{D}. \qquad (19)$$

The "zero real characteristics" boundary ($k_{rc} = 0$, Brauner and Maron, 1992b) is employed here to define the stratified flow region. The transition criterion given by Eq. 18 is supported by limited experimental data (Brauner and Maron, 1992b). It can also be obtained in the invisible Kelvin-Helmholtz analysis (Trallero, 1995). It should be noted that this criterion is not a final recommendation for predicting flow-regime transition. It is used here only as a reasonable assumption to demonstrate the ability of the proposed model to simulate the flow-regime transitions in unsteady liquid–liquid flow. Any other criteria for transition can be incorporated into the model, depending on a specific problem to be solved.

## Inhibitor Transport Model

The transport of an inhibitor in the pipeline is governed by the inhibitor mass conservation equation

$$\frac{\partial}{\partial t}(\rho_k \alpha_k y_k) + \frac{\partial}{\partial x}(\rho_k \alpha_k y_k U_k) = \Gamma_k, \quad k = a, b. \qquad (20)$$

If the inhibitor injected into the pipeline does not affect the viscosity of liquids, the inhibitor concentration and velocity of phases are uncoupled. Thus, Eq. 20 can be solved separately from the two-phase flow equations.

A conservative formulation of the inhibitor mass conservation equation can be obtained in the following form:

$$\frac{\partial y_k}{\partial t} + \frac{1}{\alpha_k}\frac{\partial}{\partial x}(\alpha_k y_k U_k) + \frac{y_k}{\alpha_k}\frac{\partial \alpha_k}{\partial t} = \frac{\Gamma_k}{\alpha_k \rho_k}, \quad k = a, b. \qquad (21)$$

The source term $\Gamma_k$ describes the transfer of the inhibitor from one phase to the other. This term can be used to model the transient partitioning of the inhibitor between the two phases. Source term $\Gamma_k$ can also be used to account for the effect of inhibitor degradation if the inhibitor is not a stable substance. In this case, corresponding constitutive relationships need to be specified to complete the formulation of the problem.

## Numerical Method

The system of governing equations, Eqs. 7, 9, and 12, was reduced to a single partial differential equation (the continuity equation for the water phase, Eq. 7) in the conservation form. This equation is a wave equation in which the water velocity is a highly nonlinear function of water holdup. The holdup wave equation, Eq. 7, can be solved numerically using either the method of characteristics or a finite difference method. As the velocity of water phase depends strongly on water holdup, a fixed grid cannot be used in the method of characteristics. The fixed grid requires interpolations at each time step, which can smooth out the sharp peaks. To avoid interpolations, a flexible grid can be used. However, if a shock is formed, the characteristic curves intersect and the method of characteristics fails (Chaudhry, 1979). This difficulty can be overcome by isolating the shock; however, the use of this procedure is not a simple task in the analysis of complex systems. Moreover, the application of the method of characteristics to the analysis of liquid–liquid flows, in which the transition from stratified to nonstratified flow pattern occurs, requires the solution of stiff equations, since the water holdup propagation speed strongly depends on the flow regime. Therefore, Eq. 7, along with boundary conditions Eqs. 16 and 17, is solved here using an explicit finite difference scheme. The pipeline is divided into a number of control volumes (mesh cells). All the flow parameters, including the velocity of phases, are defined at the cell centers. The finite difference form of Eq. 7 using forward-time and backward-space differences is

$$\frac{\alpha_{b,i}^{n+1} - \alpha_{b,i}^{n}}{\Delta t} = -\frac{(\alpha_b U_b)_i^n - (\alpha_b U_b)_{i-1}^n}{\Delta x}. \qquad (22)$$

The algebraic equations, Eqs. 9 and 12, have been brought into a single nonlinear equation of type $f(x) = 0$, which calculates $U_b$ for a given value of $\alpha_b$. This equation is solved using a standard numerical procedure (the bisection method).

The time step was limited by the Courant-Friedrichs-Lewy stability condition

$$c = \frac{V_w \Delta t}{\Delta x} \le 1. \qquad (23)$$

The one-sided or upwind differencing scheme used in the present study introduces an additional diffusion term, which is not present in the original differential equation. To minimize the effect of the artificial viscosity on the solution in the examples presented below, the time step and the mesh spacing were chosen so that the Courant number was maintained close to unity. An attempt has been made to use the Lax-Wendroff two-step scheme, which is of second-order accuracy. The solutions obtained by using the Lax-Wendroff scheme show some nonphysical oscillations, in particular, in flow-rate transients in which flow-pattern transitions occur. The use of second-order methods for solving the problem of transient liquid–liquid flow in pipes requires further study.

The finite difference equation of inhibitor transport is formulated as follows:

$$\frac{y_{k,i}^{n+1} - y_{k,i}^{n}}{\Delta t} = -\frac{1}{\alpha_{k,i}^{n}} \frac{(\alpha_k y_k U_k)_i^n - (\alpha_k y_k U_k)_{i-1}^n}{\Delta x} - \frac{y_{k,i}^{n}}{\alpha_{k,i}^{n}} \frac{\alpha_{k,i}^{n+1} - \alpha_{k,i}^{n}}{\Delta t} + \frac{\Gamma_{k,i}^{n}}{\alpha_{k,i}^{n} \rho_k}. \quad (24)$$

The only unknown variable in Eq. 24 is $y_{k,i}^{n+1}$, as the fluid flow model calculates separately the remaining variables.

## Simulation Results and Discussion

The major objective of the present work is to present a mathematical formulation for modeling the transient flow of two immiscible liquids in horizontal or slightly inclined pipes. The application of the proposed formulation to the analysis of specific situations will require closure relationships, which are determined by the conditions of the problem to be solved. In this section, the mathematical model developed is used in order to study transient oil–water flow in a long pipeline. An example of the model application to the analysis of the inhibitor transport is given.

### *Flow simulation*

A horizontal pipeline carrying an oil–water mixture ($\rho_a = 854$ kg/m$^3$, $\rho_b = 1{,}000$ kg/m$^3$, $\mu_a = 8 \times 10^{-3}$ Pa·s, and $\mu_b = 1 \times 10^{-3}$ Pa·s) has been used for numerical simulations. The length of the pipeline is 20 km, and its internal diameter is 0.3653 m (a 16-in. schedule 80 pipe). It is assumed that oil and water do not form stable water-in-oil emulsion, for example, due to the injection of a demulsifier into the line. The pipeline numerical model uses 200 mesh cells of equal length. A further increase in the number of cells did not have any significant effect on the results of calculations. Typical flow-rate transients (increasing water flow rate, decreasing water flow rate) in the pipeline have been analyzed.

Figure 3 shows the predicted water holdup for a transient in which the water superficial velocity at the entrance to the pipeline increases linearly with time from 0.1 to 0.3 m/s during 1 h. The mixture velocity is maintained constant at 2.6 m/s. The time step used in this calculation is 30 s. The flow is dispersed throughout the whole transient. As can be observed, the increase in the water flow rate at the entrance produces a water holdup wave (a density wave), which propagates through the pipeline. Distortion of the wavefront does not occur. This can be explained by examining Eq. 7. In the present study the homogeneous model is employed to describe dispersed oil–water flow. In the homogeneous flow, the velocity of the water phase does not depend on the water holdup. It is equal to the mixture (homogeneous) velocity. In the considered case, the mixture velocity is kept constant, hence the water holdup wave propagates at a constant speed.

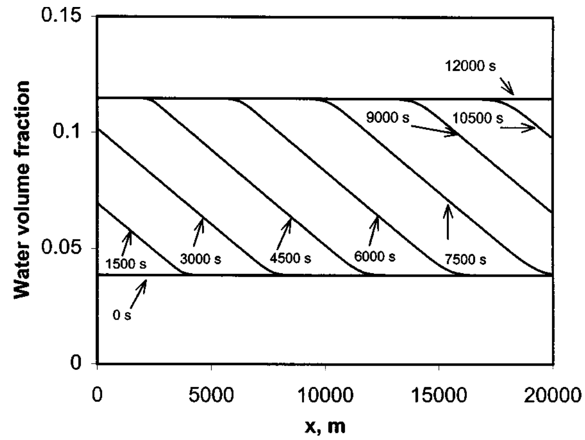


**Figure 3. Water holdup wave propagation (dispersed flow).**

The results presented in Figures 4 and 5 show the effect of a decrease in the inlet water superficial velocity in stratified oil–water flow. The water superficial velocity at the pipeline entrance decreases linearly with time from 0.2 m/s to 0.05 m/s during 1 h. The mixture velocity is maintained at 1 m/s. Figure 4 shows the transient water volume fraction profiles. The water holdup wave is deformed as the wave travels through the pipeline. In stratified flow the water velocity depends strongly on the water volume fraction (Eq. 12). A decrease in the water volume fraction results in a decrease in the velocity of the water phase (Figure 5). At the wavefront, a particle of water at an upstream location has a higher velocity than one at a downstream location. This leads to the smoothening of the wavefront.

Figures 6 and 7 shows transient water holdup and velocity profiles, respectively, for a transient in which the inlet water superficial velocity is gradually increased from 0.05 m/s to

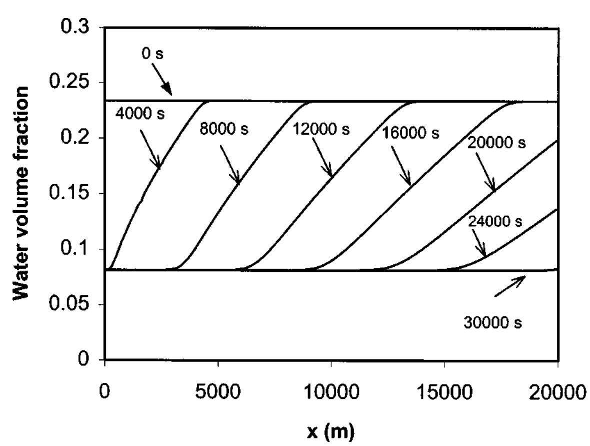


**Figure 4. Water holdup wave propagation (stratified flow, decreasing water flow rate).**

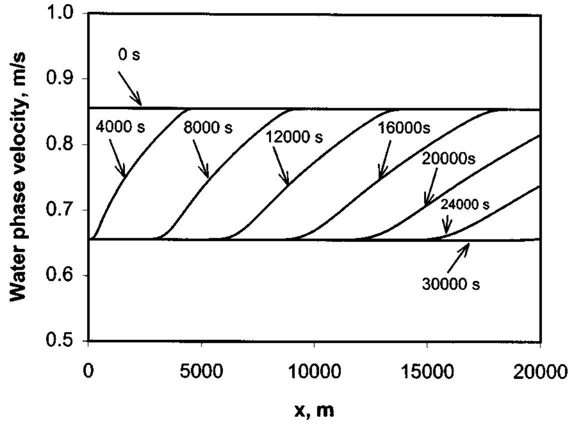


**Figure 5. Transient water velocity profiles (stratified flow, decreasing water flow rate).**

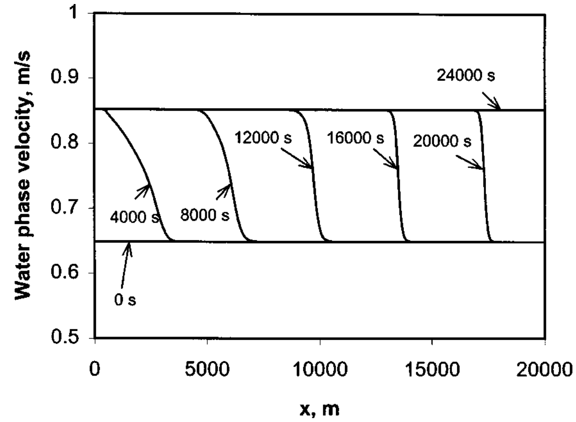


**Figure 7. Transient water velocity profiles (stratified flow, increasing water flow rate).**

0.2 m/s and the mixture velocity is kept at 1 m/s. As can be seen from Figure 6, the wavefront becomes steeper as the wave approaches the pipeline outlet. Contrary to the preceding case, a particle of water at a downstream location at the wavefront has a higher velocity than one at an upstream location (Figure 7). This phenomenon can lead to the formation of a normal-shock wave (an abrupt change in the water holdup). In the example presented here, the shock is formed at $t \approx 20{,}000$ s. The formation of shocks in vertical oil–water flow was found by Asheim and Grodal (1998). They also showed that in a transient caused by a decrease in the input water volume fraction leads to the smoothening of the holdup wavefront. The results presented in the present study show that analogous phenomena occur in horizontal stratified liquid–liquid flow during transients caused by large variations of the oil and water flow rates at the entrance to the pipeline.

In the last case considered here, the effect of the pipe inclination of the flow behavior has been studied. A 20-km-long 16-in.-diameter schedule 80 pipeline is divided into four sections of equal length, as shown in Figure 8. The first and the fourth sections are horizontal. The second and the third sections are inclined 2° upward and 2° downward, respectively. Initially, steady-state flow is assumed along the pipeline, with

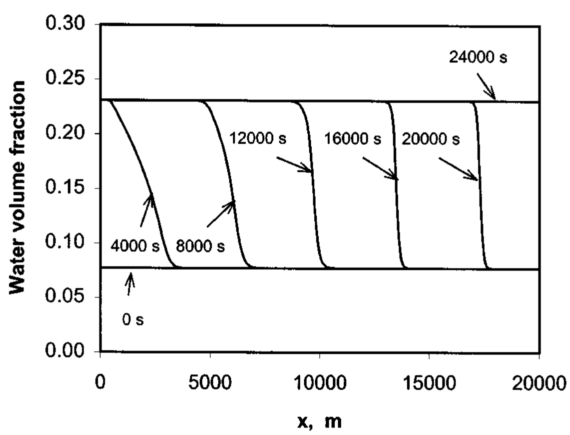


**Figure 6. Water holdup wave propagation (stratified flow, increasing water flow rate).**

$U_m = 1$ m/s and $U_b = 0.05$ m/s. Figures 9 and 10 show the response of the system on an increase in the inlet superficial water velocity from 0.05 m/s to 0.2 m/s. As in the cases considered earlier, the water flow rate is increased linearly with time during 1 h and the mixture velocity is kept constant at the initial value. At $t = 0$ s, the flow pattern is stratified flow in all four sections of the pipeline. Due to the gravity effect, water flows slower in the upward-sloping section and faster in the downward-sloping section as compared to water flowing in the horizontal sections (Figure 10). The initial water holdup distribution along the pipeline (Figure 9) corresponds to this water-velocity profile. At $t = 3000$ s, a water holdup wave propagates downstream in the first section of the pipeline. The water holdup wave becomes steeper in the process of wave propagation through the first section. This phenomenon was discussed earlier in the analysis of the transient produced by an increasing water flow rate in a horizontal pipeline. At about 6000 s, the wavefront reaches the second section. Water is accumulated at the bend joining the first section with the second one. The water accumulation at the bend produces a "hump" on the water holdup plot. At $t = 9000$ s, a rise of the water level at the second section results in the transition to dispersed flow. This transition occurs in the wavefront when $\alpha_b \approx 0.17$. An evidence of this is the fact that the water velocity here is equal to the mixture velocity (Figure 10). The change of the flow regime leads to the formation of a small, near-horizontal section on the water holdup plot, which is subsequently pushed toward the pipeline outlet. In the third section (Figure 9), the flow remains stratified and the water accumulation rate is limited by the acceleration of the water flow: water is a denser liquid than oil; thus, the gravity force has a larger effect on the water velocity than on the oil velocity. At 12,000 s, the accumulation of water at the second bend produces another "hump" on the water holdup profile plot. In the first and the third sections, the flow pattern is stratified flow. Dispersed flow takes place in the second section. The first section and most of the second are in steady state. At $t = 13{,}500$ s, further water accumulation at the second bend occurs and water continues to displace oil from the fourth section. At $t = 16{,}500$ s, the holdup wavefront reaches the pipeline exit. At $t = 19{,}500$ s, steady-state flow is established in the first three sec-

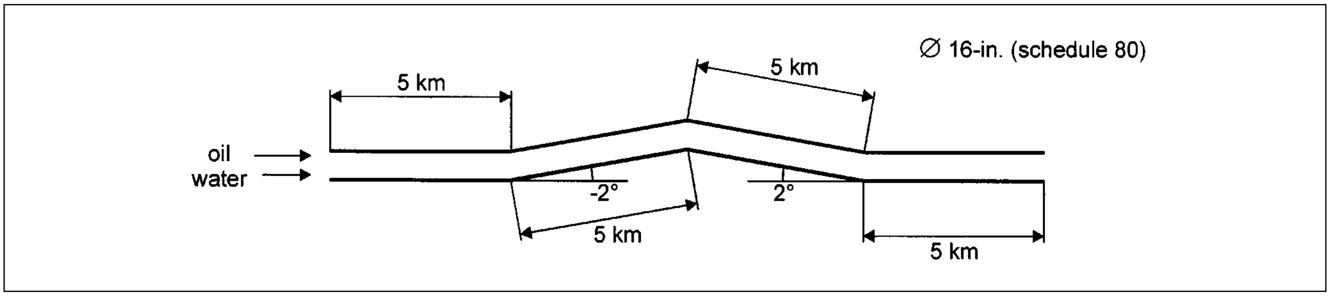


**Figure 8. Pipeline configuration.**

tions of the pipeline, while in the fourth section a further increase in the water holdup occurs. Finally, at $t = 24{,}000$ s, a new steady state is reached along the whole length of the pipeline. The flow pattern in the pipeline is mostly stratified flow, except for the upward-sloping section where dispersed flow prevails.

In this study, it was not possible to demonstrate predictive capability of the model, because of the lack of experimental or field data on transient liquid–liquid flow in horizontal pipes. The main purpose of this work is to present a mathematical model for solving problems involving the unsteady flow of two immiscible liquids in pipes. It should be pointed out here that the required accuracy of a particular model can be achieved by the use of appropriate closure relationships, as is done in all the previously mentioned computer codes.

### *Inhibitor transport simulation*

Continuous injection of a corrosion inhibitor into the pipeline considered in the previous section has been modeled. A simple case has been analyzed. The inhibitor is assumed to be soluble in water, and the effect of partitioning the inhibitor between the oil and water phases is negligible ($\Gamma_b = 0$). It is also assumed that the inhibitor degradation does not occur. The inhibitor dilution in a pipeline due to an increase in the water rate at the entrance has been simulated. The geometry of the pipeline, the boundary, and initial conditions are the same as in the last case considered in the previous section. Initially, the inhibitor concentration is uniform along the pipeline, with $y_b = 95$ ppm (mg/L). The simulation results are shown in Figure 11. A concentration wave propagates downstream. As can be seen, the concentration wave-propagation speed varies. It decreases when the wave reaches the first bend where water accumulation occurs (see Figures 9 and 10). The propagation speed increases when the wave travels through the second and the third sections. Here, the slope of the wave front relatively horizontal, decreases. This can be attributed to an increase in water velocity (Figure 10). The water phase slows down at the third bend in the pipe. The water slowdown results in a decrease in the concentration wave propagation speed. The slope of the wavefront increases. At $t = 23{,}000$ s, a new steady-state concentration profile is established along the pipeline.

It should be noted that the considered example is the simplest case of the inhibitor transport conditions. If the partitioning effect is not negligible ($\Gamma_b \neq 0$), the inhibitor behavior will be much more complex. In this case, the proposed numerical algorithm can be adapted for solving particular problems by specifying corresponding constitutive relationships.

## Conclusions

A two-fluid model for the transient flow of two immiscible liquids in a pipeline has been developed. The model is based on two transient continuity equations and a combined momentum equation in quasi-steady form. The model is able to simulate both stratified and dispersed flow patterns. A study

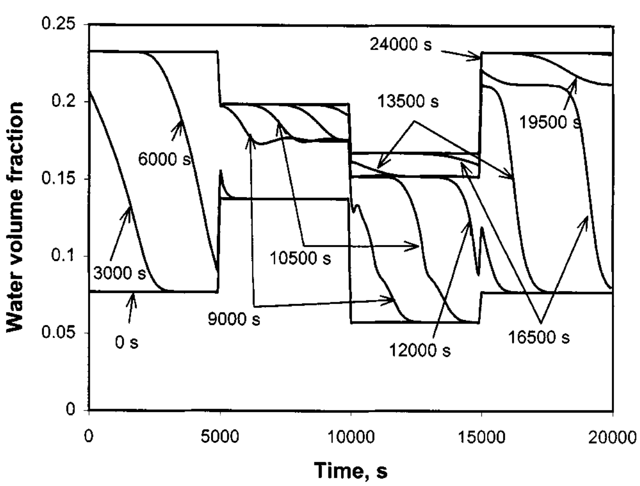


**Figure 9. Transient water holdup distributions.**

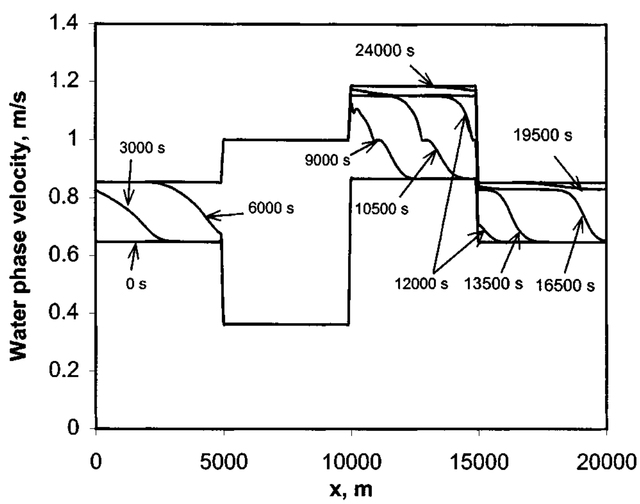


**Figure 10. Transient water velocity profiles.**

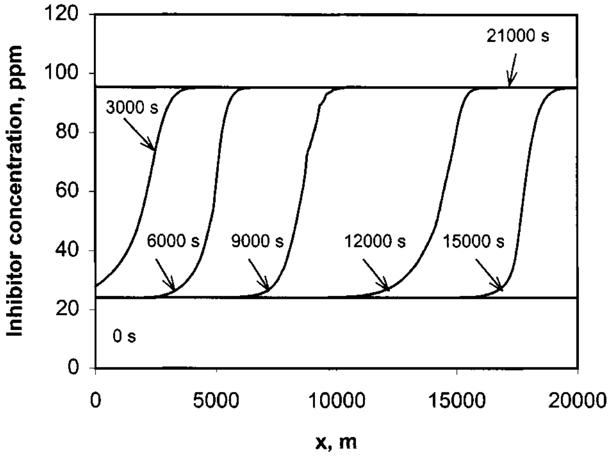


**Figure 11. Concentration wave propagation in water.**

of transient oil−water flow in a horizontal or slightly inclined pipe has been carried out. The results obtained show that a gradual increase in the input water fraction in horizontal stratified liquid−liquid flow may result in the formation of a normal shock. The decreasing water flow rate leads to the smoothening of the holdup wave. This flow behavior is explained by a strong dependence of the holdup wave propagation speed on the water holdup. An experimental study needs to be carried out to confirm these theoretical results. The developed model has been used to simulate the transport of a corrosion inhibitor in a pipeline conveying an oil−water mixture. It has been found that the dynamics of liquid−liquid two-phase flow has a significant effect upon the inhibitor concentration distribution in a phase. The results presented in this study improve the understanding of transient liquid−liquid flow and of inhibitor transport in this flow.


## Acknowledgments

The author is grateful to Dr. Moises Berezowsky for valuable discussions on the choice of numerical method.


## Notation

$A$ = area
$D$ = pipe internal diameter
$c$ = Courant number
$g$ = acceleration due to gravity
$h$ = water-layer height
$k$ = wavenumber
$p$ = pressure
$S$ = perimeter
$t$ = time
$y$ = inhibitor concentration
$\alpha$ = volume fraction of phase (*in-situ* holdup)
$\beta$ = inclination angle
$\rho$ = density
$\sigma$ = surface tension
$\tau$ = shear stress

### Subscripts

$a$ = less dense phase (oil)
$b$ = more dense phase (water)
$e$ = entrance
$i$ = interface
$k$ = phase
$s$ = superficial
0 = initial

## Literature Cited


Angeli, P., and G. F. Hewitt, "Pressure Gradients in Horizontal Liquid-Liquid Flows," *Int. J. Multiphase Flow*, **24**, 1183 (1998).

Asheim, H., and E. Grodal, "Holdup Propagation Predicted by Steady-State Drift Flux Models," *Int. J. Multiphase Flow*, **24**, 757 (1998).

Bendiksen, K., D. Malnes, R. Moe, and S. Nuland, "The Dynamic Two-Fluid Model OLGS: Theory and Application," *SPE Prod. Eng.*, **6**, 171 (1991).

Black, P. S., L. C. Daniels, N. N. Hoyle, and W. P. Jepson, "Studying Transient Multiphase Flow Using the Pipeline Analysis Code (PLAC)," *J. Energy Resour. Technol.*, **112**, 25 (1990).

Brauner, N., and D. M. Maron, "Stability Analysis of Stratified Liquid-Liquid Flow," *Int. J. Multiphase Flow*, **18**, 103 (1992a).

Brauner, N., and D. M. Maron, "Flow Pattern Transitions in Two-Phase Liquid-Liquid Flow in Horizontal Tubes," *Int. J. Multiphase Flow*, **18**, 123 (1992b).

Brauner, N., and D. M. Maron, "The Role of Interfacial Shear Modelling in Predicting Stability of Stratified Two-Phase Flow," *Chem. Eng. Sci.*, **48**, 2867 (1993c).

Chaudhry, M. H., *Applied Hydraulic Transients*, Van Nostrand Reinhold, New York (1979).

Erikckson, D., E. Buck, and J. Kolts, "Corrosion Inhibitor Transport in a Wet-Gas Pipeline," *Mater. Performance*, **13**, 49 (1993).

Flores, J. G., C. Sarica, T. X. Chen, and J. P. Brill, "Investigation of Holdup and Pressure Drop Behavior for Oil-Water Flow in Vertical and Deviated Wells," *J. Energy Resour. Technol.*, **120**, 8 (1998).

Jackson, J. F., D. R. Liles, V. H. Ransom, and L. J. Ybarrondo, "LWR System Safety Analysis," *Nuclear Reactor Safety Heat Transfer*, O. C. Jones, ed., Hemisphere, New York, p. 415 (1981).

Masella, J. M., Q. H. Tran, D. Ferre, and C. Pauchon, "Transient Simulation of Two-Phase Flow in Pipes," *Int. J. Multiphase Flow*, **24**, 739 (1998).

Reibold, W. L., M. Reocreux, and O. C. Jones, "Blowdown Phase," *Nuclear Reactor Safety Heat Transfer*, O. C. Jones, ed., Hemisphere, New York p. 415 (1981).

Ricca, P. M., "Ultrasonic Inspection Prompts of Chemical Inhibitor Program," *Oil & Gas J.*, 73 (1991).

Taitel, Y., and D. Barnea, "Simplified Transient Simulation of Two Phase Flow Using Quasi-Equilibrium Momentum Balances," *Int. J. Multiphase Flow*, **23**, 493 (1997).

Trallero, J. L., "Oil-Water Flow Patterns in Horizontal Pipes," PhD Diss., The Univ. of Tulsa, Tulsa, OK (1995).

Wallis, G. B., "Review—Theoretical Models of Gas-Liquid Flows," *J. Fluid Eng.*, **104**, 279 (1982).

Zuber, N., and J. Findlay, "Average Volumetric Concentration in Two-Phase Flow Systems," *J. Heat Transfer*, Ser. C, **87**, 453 (1965).



*Manuscript received Apr. 16, 1999, and revision received Dec. 17, 1999.*